



The NESSiE way to searches for sterile neutrinos at FNAL

L. Stanco, for the NESSiE Collaboration

INFN-Padova, Via Marzolo, 8 I-35131 Padova, Italy

Abstract

Neutrino physics is nowadays receiving more and more attention as a possible source of information for the long-standing problem of new physics beyond the Standard Model. The recent measurement of the mixing angle θ_{13} in the standard mixing oscillation scenario encourages us to pursue the still missing results on leptonic CP violation and absolute neutrino masses. However, puzzling measurements exist that deserve an exhaustive evaluation.

The NESSiE Collaboration has been setup to undertake conclusive experiments to clarify the *muon–neutrino disappearance* measurements at small L/E , which will be able to put severe constraints to models with more than the three-standard neutrinos, or even to robustly measure the presence of a new kind of neutrino oscillation for the first time. To this aim the use of the current FNAL–Booster neutrino beam for a Short–Baseline experiment has been carefully evaluated. Its recent proposal refers to the use of magnetic spectrometers at two different sites, Near and Far ones. Their positions have been extensively studied, together with the possible performances of two OPERA–like spectrometers. The proposal is constrained by availability of existing hardware and a time–schedule compatible with the undergoing project of a multi–site Liquid–Argon detectors at FNAL.

The experiment to be possibly setup at Booster will allow to definitively clarify the current ν_{μ} disappearance tension with ν_e appearance and disappearance at the eV mass scale.

Keywords: BSM, Neutrino, Sterile, Interactions, Beams

The NESSiE Collaboration for the FNAL experiment

A. Anokhina¹¹, A. Bagulya¹⁰, M. Benettoni¹², P. Bernardini^{8,7}, R. Brugnera^{13,12}, M. Calabrese⁷, A. Cecchetti⁶, S. Cecchini³, M. Chernyavskiy¹⁰, P. Creti⁷, F. Dal Corso¹², O. Dalkarov¹⁰, A. Del Prete^{9,7}, G. De Robertis¹, M. De Serio^{2,1}, L. Degli Esposti³, D. Di Ferdinando³, S. Dusini¹², T. Dzhatdov¹¹, C. Fanin¹², R. A. Fini¹, G. Fiore⁷, A. Garfagnini^{13,12}, S. Golovanov¹⁰, M. Guerzoni³, B. Klicek¹⁵, U. Kose⁵, K. Jakovcic¹⁵, G. Laurenti³, I. Lippi¹², F. Loddo¹, A. Longhin⁶, M. Malenica¹⁵, G. Mancarella^{8,7}, G. Mandrioli³, A. Margiotta^{4,3}, G. Marsella^{8,7}, N. Mauri⁶, E. Medinaceli^{13,12}, A. Mengucci⁶, R. Mingazheva¹⁰, O. Morgunova¹¹, M. T. Muciaccia^{2,1}, M. Nessi⁵, D. Orecchini⁶, A. Paoloni⁶, G. Papadia^{9,7}, L. Paparella^{2,1}, L. Pasqualini^{4,3}, A. Pastore¹, L. Patrizii³, N. Polukhina¹⁰, M. Pozzato^{4,3}, M. Roda^{13,12}, T. Roganova¹¹, G. Rosa¹⁴, Z. Sahnoun^{3‡}, S. Simone^{2,1}, C. Sirignano^{13,12}, G. Sirri³, M. Spurio^{4,3}, L. Stanco^{12,a}, N. Starkov¹⁰, M. Stipcevic¹⁵, A. Surdo⁷, M. Tenti^{4,3}, V. Togo³, M. Ventura⁶ and M. Vladymyrov¹⁰.

(a) Spokesperson

1. INFN, Sezione di Bari, 70126 Bari, Italy

2. Dipartimento di Fisica dell'Università di Bari, 70126 Bari, Italy

3. INFN, Sezione di Bologna, 40127 Bologna, Italy

4. Dipartimento di Fisica e Astronomia dell'Università di Bologna, 40127 Bologna, Italy

5. European Organization for Nuclear Research (CERN), Geneva, Switzerland

6. Laboratori Nazionali di Frascati dell'INFN, 00044 Frascati (Roma), Italy

7. INFN, Sezione di Lecce, 73100 Lecce, Italy

8. Dipartimento di Matematica e Fisica dell'Università del Salento, 73100 Lecce, Italy

9. Dipartimento di Ingegneria dell'Innovazione dell'Università del Salento, 73100 Lecce, Italy

10. Lebedev Physical Institute of Russian Academy of Science, Leninskie pr., 53, 119333 Moscow, Russia.

11. Lomonosov Moscow State University (MSU SINP), 1(2) Leninskie gory, GSP-1, 119991 Moscow, Russia

12. INFN, Sezione di Padova, 35131 Padova, Italy

13. Dipartimento di Fisica e Astronomia dell'Università di Padova, 35131 Padova, Italy

14. Dipartimento di Fisica dell'Università di Roma "La Sapienza" and INFN, 00185 Roma, Italy

15. Rudjer Boskovic Institute, Bijenicka 54, 10002 Zagreb, Croatia

‡ Also at Centre de Recherche en Astronomie Astrophysique et Geophysique, Alger, Algeria

1. Introduction and Physics Overview

The unfolding of the physics of the neutrino is a long and exciting history spanning the last 80 years. Over this time the interchange of theoretical hypotheses and experimental facts has been one of the most fruitful demonstrations of the progress of knowledge in physics. The work of the last decade and a half finally brought a coherent picture within the Standard Model (SM) (or some small extensions of it), namely the mixing of three neutrino flavour states with three ν_1 , ν_2 and ν_3 mass eigenstates. The last unknown mixing angle, θ_{13} , was recently measured [1] but still many questions remain unanswered to completely settle the scenario: the absolute masses, the Majorana/Dirac nature and the existence and magnitude of leptonic CP violation. Answers to these questions will beautifully complete the (standard) three–neutrino model but they will hardly provide an insight into new physics Beyond the Standard Model (BSM). Many relevant questions will stay open: the reason for the characteristic nature of neutrinos, the relation between the leptonic and hadronic sectors of the SM, the origin of Dark Matter and, overall, where and how to look for BSM physics. Neutrinos may be an excellent source of BSM physics and their history is supporting that at length.

There are actually several experimental hints for deviations from the “coherent” picture described above. Many unexpected results, not statistically significant on a single basis, appeared also in the last decade and a half, bringing attention to the hypothesis of the existence of *sterile neutrinos* [2]. A White Paper [3], contains a comprehensive review of these issues. In particular we would like to focus on tensions in many phenomenological models that grew up with experimental results on neutrino/antineutrino oscillations at Short–Baseline (SBL) and with the more recent, carefully recomputed, antineutrino fluxes from nuclear reactors. The main source of tension corresponds to the lack so far of any ν_μ disappearance signal [4]. This tension has been strengthened by the recent exclusion limits reported at the NEUTRINO2014 conference [5].

This scenario promoted several proposals for new, exhaustive evaluations of the neutrino behaviour at SBL. Since the end of 2012 CERN is undergoing a study to setup a Neutrino Platform, with a new infrastructure at the North Area that, for the time being, will not include a new neutrino beam [6]. Meanwhile FNAL is welcoming proposals of experiments to exploit the physics potentials of their two existing neutrino beams, the Booster and the NUMI beams, following the recent recommendations from USA HEP-P5 report [7]. Two recent proposals [10, 9] have been submitted for experiments of SBL at the Booster beam, to complement the about to start MicroBooNE experiment [8]. They are both based on the Liquid Argon technology and aim to measure the ν_e appearance at SBL, with possibilities to study the ν_μ disappearance. Possible use of magnetic spectrometers at two different sites at FNAL–Booster beam have been proposed by the NESSiE collaboration and discussed in detail in [11].

The NESSiE proposal is based on the following considerations:

- the measurement of ν_μ spectrum and trend is mandatory for a correct interpretation of the ν_e data, even in case of a null result for the latter;
- a decoupled measurement of ν_e and ν_μ interactions will allow to reach in the analyses the percent–level systematics due to the different cross–sections;
- very massive detectors are mandatory to collect a large number of events thus improving the disentangling of systematic effects.
- limited experimental data are available on ν_μ disappearance at SBL: the dated CDHS experiment [12] and the more recent results from MiniBooNE [13], a joint MiniBooNE/SciBooNE analysis [14] and MINOS and SK [5]. The latter results slightly extend the ν_μ disappearance exclusion region set by CDHS. Fig. 1 shows the excluded regions in the space parameters for the $\nu_\mu \rightarrow \nu_s$ oscillation, obtained through ν_μ disappearance experiments. The mixing angle is denoted as θ_{new} and the squared mass difference as Δm_{new}^2 . The region with $\sin^2(2\theta_{new}) < 0.1$ is largely still unconstrained.

2. Proposal for the FNAL–Booster

Motivated by the present scenario a detailed study of the physics case for the FNAL–Booster beam was performed. The study follows the similar analysis developed for the CERN–PS and CERN–SPS cases [16, 17] and the study in [18]. We pondered many detector configurations investigating experimental aspects not fully addressed by

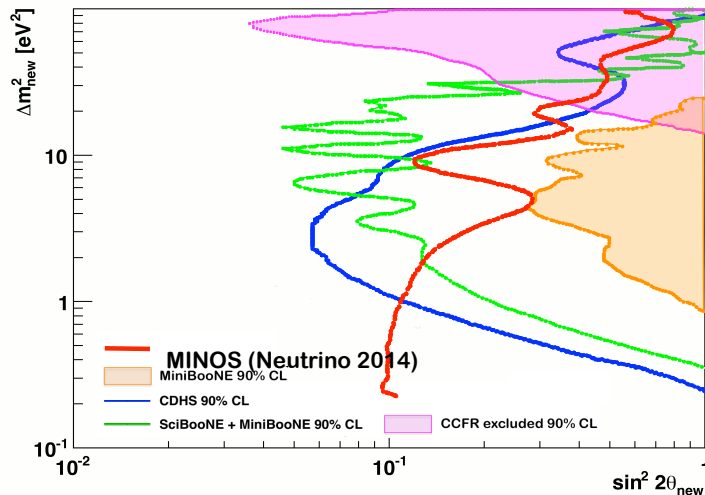


Figure 1: The current exclusion limits on the ν_μ disappearance searches at the eV^2 scale. Blue (green) line: old (recent) exclusion limits on ν_μ from previous CDHS [12] and recent MiniBooNE/SciBooNE [14] measurements. The two filled areas correspond to the exclusion limits on the $\bar{\nu}_\mu$ from CCFR [15] and MiniBooNE-alone [13] experiments (at 90% C.L.). The red curve corresponds to the very recent result from MINOS [5].

the LAr detection. This includes the measurements of the lepton charge on event-by-event basis and its energy over a wide range. Indeed, muons from Charged Current (CC) neutrino interactions play an important role in disentangling different phenomenological scenarios provided their charge state is determined. Also, the study of muon appearance/disappearance can benefit from the large statistics of muonic-CC events from the primary neutrino beam. In the FNAL-Booster beam the antineutrino contribution is rather small and it then becomes a systematic effect to be taken into account.

Results of our study are reported in detail in the full NESSiE proposal [11]. We aim to design, construct and install two spectrometers at two sites, “Near” (at 110 m, on-axis) and “Far” (at 710 m, on surface), in line with the FNAL-Booster, fully compatible with the proposed LAr detectors. Profiting of the large mass of the two spectrometer-systems, their stand-alone performances are exploited for the ν_μ disappearance study. Besides, complementary measurements with LAr can be undertaken to increase their control of systematic errors.

Some important practical constraints were assumed in order to draft a proposal on a conservative, manageable basis, with sustainable timescale and cost-wise. Well known technologies were considered as well as re-using large parts of existing detectors.

The momentum and charge state measurements of muons in a wide range, from few hundreds MeV/c to several GeV/c, over a $> 50 \text{ m}^2$ surface, is an extremely challenging task if constrained by an order of 1 million € budget for construction and installation. Running costs must be kept at low level, too.

We believe to have succeeded in developing a substantial proposal that, by keeping the systematic error at the level of $1 \div 2\%$ for the measurements of the ν_μ interactions, will allow to:

- measure ν_μ disappearance in the almost entire available momentum range ($p_\mu \geq 500 \text{ MeV}/c$). The capability in rejecting/observing the anomalies over the whole expected parameter space of sterile neutrino oscillations is a key feature, since the momentum range corresponds to an almost equivalent Δm_{new}^2 interval;
- collect a very large statistical sample in order to span the oscillation mixing parameter down to till un-explored regions ($\sin^2(2\theta_{new}) \gtrsim 0.01$);
- measure the neutrino flux at the Near detector, in the relevant muon momentum range, to keep the systematic errors at the lowest possible values;
- measure the sign of the muon charge to separate ν_μ from $\bar{\nu}_\mu$ for systematics control.

In the following the key points of the proposal are recalled.

2.1. The Booster Neutrino Beam (BNB)

The neutrino beam [19] is produced using protons with a kinetic energy of 8 GeV extracted from the Booster and directed to a Beryllium cylindrical target with a length of 71 cm and 1 cm diameter. The target is surrounded by a magnetic focusing horn pulsed with a 170 kA current at a rate of 5 Hz. Secondary mesons are projected into a 50 m long decay pipe where they are allowed to decay in flight before reaching by an absorber and the ground material. An additional absorber can be placed in the decay pipe at about 25 m from the target¹. Neutrinos travel about horizontally at a depth of about 7 m underground.

A booster acceleration cycle typically contains about 4.5×10^{12} protons. Batches have a duration of 1.6 μ s and are subdivided into 84 bunches, about 4 ns wide and spaced by about 19 ns. The rate of batch extraction is limited by the horn pulsing at 5 Hz. This timing structure provides a very powerful handle to constraint background from cosmic rays.

2.2. The Far-to-Near ratio (FNR)

The uncertainty on the absolute ν_μ flux at MiniBooNE stays below 20% for energies below 1.5 GeV while it increases drastically above that energy. The uncertainty is dominated by the knowledge of hadronic interactions of protons on the Be target, which affects the angular and momentum spectra of neutrino parents emerging from the target. The obtained result [19] is based on experimental data obtained by the HARP and E910 collaborations.

Such a large uncertainty makes the use of two or more identical detectors at different baselines mandatory when searching for small disappearance phenomena. The ratio of the event rates at the Far and Near detectors (FNR) as function of neutrino energy is a convenient variable since it benefits at first order from cancellation of common proton–target and neutrino cross–sections systematics and of the effects of reconstruction efficiencies.

Thanks to these cancellations the uncertainty on the FNR or, equivalently, on the Far spectrum extrapolated from the Near spectrum is usually at the percent level ranging in the 0.5–5.0% interval.

It can be noted that, even in the absence of oscillations, the energy spectra in the two detectors are different, thus leading to a non–flat FNR. This is especially true if the Near detector is at a distance comparable to the length of the decay pipe. It is therefore essential to master the knowledge of the FNR for physics searches.

Compared to the Far site the solid angle subtended by the Near detector is larger. Moreover neutrinos originating from meson decays at the end of the decay pipe have a larger probability of being detected. On the contrary, only neutrinos produced in a narrow forward cone will cross the Far detector.

Assuming realistic detector sizes (see Table 2) the effect of the increased acceptance of the Near detector for neutrinos from late decays is illustrated in Fig. 2. The ratio of the distributions of the neutrino production points (radius R vs longitudinal coordinate Z) is shown for a sample crossing a Near and a Far detector placed at 110 and 710 m from the target, respectively. Neutrinos produced at large Z can be detected in the Near detector even if produced at relatively large angles, thus enhancing the low energy part of the spectrum. On the other hand neutrinos coming from meson decays late in the decay pipe are originating from the fast pion component which is more forward–boosted. The former effect is the leading one so the net effect is a softer neutrino energy spectrum at the Near site.

From these qualitative considerations it becomes clear that the prediction of the FNR is a delicate task requiring a full simulation of the neutrino beamline and of the detector acceptance, and a careful control of the systematic uncertainties.

All the contributions to the systematic uncertainties have been studied in detail by the MiniBooNE collaboration in [19]. The dominant contribution comes from the knowledge of the hadroproduction double differential (p , θ) cross–sections in 8 GeV p –Be interactions. At first order these contributions factorize out using a double site.

In order to understand how the hadroproduction uncertainty affects the accuracy on FNR for the specific case of our experiment we developed anew the beamline simulation. The angular and momentum distribution of pions exiting the Be target were studied using:

- FLUKA 2011.2b [20],
- GEANT4 (v4.9.4 p02, QGSP 3.4 physics list),

¹This configuration, which is not currently in use, could eventually alter the beam properties (i.e. providing a more point–like source for the Near site) thus allowing for extra experimental constraints on the systematic errors.

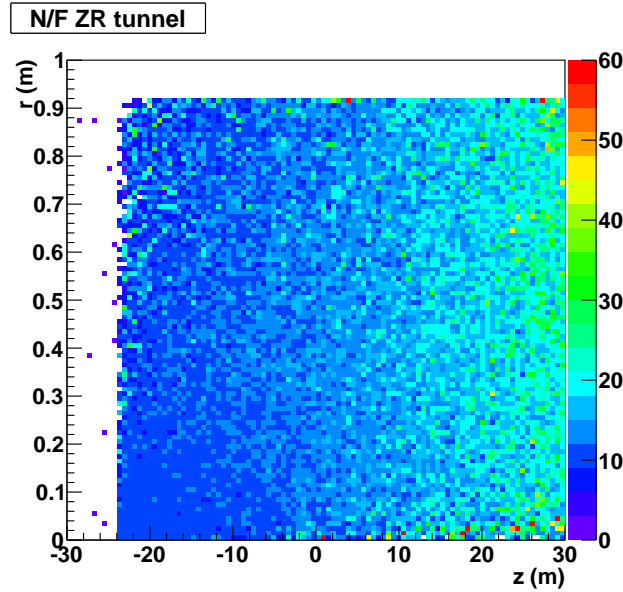


Figure 2: Ratio between the Z–R distributions of neutrino production points for neutrinos observed in a Near detector (at 110 m) over neutrinos observed in a Far detector (at 710 m). Two effects are most relevant: there is no apparent dependence on the radial R distribution; and, as expected, the Near detector has a higher acceptance for neutrinos produced in the most downstream part of the decay pipe, i.e. at high Z.

config.	L_N (m)	L_F (m)	y_N (m)	y_F (m)	s_N (m)	s_F (m)
1	110	710	0	0	4	8
2	110	710	0	0	1.25	8
3	110	710	1.4	11	4	8
4	110	710	1.4	11	1.25	8
5	460	710	7	11	4	8
6	460	710	6.5	10	4	6

Table 1: Near–Far detectors configurations. $L_{N(F)}$ is the distance of the Near (Far) detector from the target. $y_{N(F)}$ is the vertical coordinate of the center of the fiducial area of the Near (Far) detector with respect to the beam axis which lies at about -7 m underneath the ground surface. $s_{N(F)}$ is the dimension of the fiducial area of the Near (Far) detector.

- a Sanford–Wang parametrization determined from a fit of the HARP and E910 data sets in [19],

$$\frac{d^2\sigma}{dpd\Omega} = c_1 p^{c_2} \left(1 - \frac{p}{p_B - 1}\right) \exp\left(-\frac{p^{c_3}}{p_B^{c_4}} - c_5 \theta (p - c_6 p_B \cos^{c_7} \theta)\right) \quad (1)$$

where p , θ are the angular and momentum distribution of pions exiting the Be target while p_B is the proton beam momentum in GeV/c.

2.3. The experimental sites

A set of six configurations were studied considering a combination of distances (110, 460 and 710 m), on–axis or off–axis configurations and different fiducial sizes of the detectors. Their geometrical parameters are given in Tab. 1. The FNRs for the six considered configurations using either FLUKA, GEANT4 or the Sanford–Wang parametrization for the simulation of p –Be interactions have been studied via several Monte Carlo samples.

Configuration 1 (with on–axis detectors and a large Near detector) produces a FNR increasing with energy as expected from the considerations presented above, and largely departing from a flat curve. By restricting the fiducial area in the Near detector (configuration 2) the FNR flattens out as expected. This behavior is also confirmed using off–axis detectors (configurations 3 and 4). Configurations with a Near detector at larger baselines (5 and 6) tend to produce flatter FNRs, as expected. The different behaviors are more easily visible in Fig. 3 where FNRs, normalized to each other, are compared (taking the Sanford–Wang parametrization).

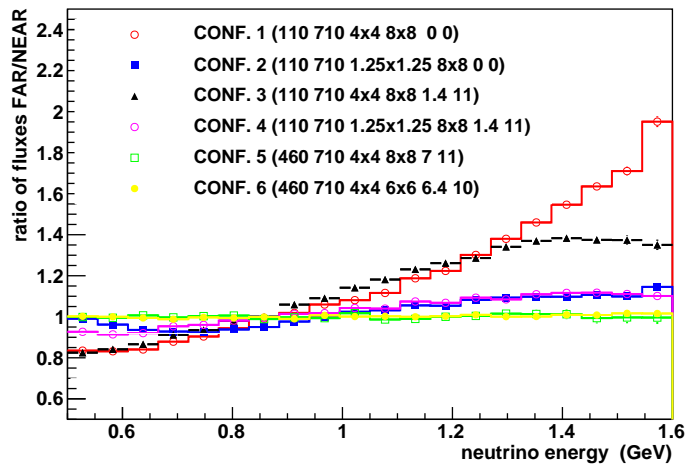


Figure 3: Far-to-Near ratios for the six considered configurations using the Sanford–Wang parametrization.

The GEANT4 and FLUKA based simulations provide results that are in agreement at a level between 1% and 3% for the configurations for which only the overlapping regions between the Far and Near detectors are considered [11]. A better estimate of the stability of FNR against hadroproduction uncertainties has been obtained using the Sanford–Wang parametrization of pion production data from HARP and E910 for the target replica. The coefficients c_i in Eq. 1 have been sampled within their uncertainties. The correlations for the uncertainties [19] have been properly taken into account using the Cholesky decomposition of the covariance matrix. The resulting uncertainties are large (5-7%) [11] when taking the full area of the Near detector at 110 m while they decrease significantly by restricting to the central region. In particular, configuration 4, which is realistic from practical considerations, has an uncertainty ranging from 2% at low energy decreasing below 1.5-0.5% for neutrino energies above 1 GeV. The uncertainty is also quite good (generally below 0.5%) for a Near site at 460 m.

In conclusion, using the constraints from HARP/E910 data sets, we estimate the uncertainties for FNR associated to hadroproduction being of the order of 1-2% for a configuration with the Far detector at surface and the Near detector at an equivalent off-axis angle and a fiducial volume tailored to match the acceptance of the Far detector (configuration 4). Given also the high available statistics and the large lever-arm for oscillation studies we consider such a layout with baselines of 110 m and 710 m as a viable choice. Of course, “configuration 4” is a subset of “configuration 3”, which could be that to be used in reality by rearranging the OPERA spectrometers (see next Section). Therefore, given the possibility for a higher statistics collection and the minor concern about the height of the pit (that has to be anyhow centered at the level of the beam) the following studies are based on “configuration 3”.

2.4. Spectrometer Design Studies

The location of the Near and Far sites corresponds a fundamental issue in the sterile neutrino search. Moreover the two detector systems at the two sites have to be as similar as possible. The NESSiE Far spectrometer has to be designed to cope with an aggressive time schedule and to largely exploit the acquired experience with the OPERA spectrometers in construction, assembling and maintenance [21]. Well known technologies have been considered as well as re-using large parts of existing detectors. The OPERA spectrometers will begin to be dismantled sometime next year and we foresee to use them all. The relatively low momentum range of muons from the BNB charged current events suggests to couple together the two OPERA spectrometers, for both the Far and the Near sites. Their modularity will allow to take 4/7 of the acceptance region (by height) for the Far site and 3/7 for the Near one. Each iron slab will be cut at 4/7 in height to reproduce exactly the Far and Near targets. In this way any inaccuracy either in geometry (the single 5 cm iron slab owns a precision of few mm) or in the material will be exactly reproduced in the two detection sites. The Near NESSiE spectrometer will then be a sacked down clone of the Far one, with identical thickness along the beam but reduced transverse size.

The performances of the current geometry with 5 cm thick iron–slabs are evaluated in terms of NC contamination and momentum resolution, and compared to a possible geometry with 2.5 cm slab thickness. Using 2.5 cm thick slabs, the fraction of neutrino interactions producing a signal in the RPCs increases for both NC and CC events. The CC efficiency and the NC contamination are both larger with respect to the reference 5 cm geometry. At the same level of purity the efficiencies in the two geometries are similar. No advantage in statistics is obtained requiring the same NC contamination suppression.

3. Physics Analysis and Performances

We developed sophisticated analyses to determine the sensitivity region that can be explored with an exposure of 6.6×10^{20} p.o.t., corresponding to 3 years of data collection at FNAL–Booster beam. Our guidelines have been the maximal extension at small values of the mixing angle parameter, as well as its dependence on systematic effects.

To this aim, three different analyses have been set up, of different complexity:

- the usual sensitivity plot based on the Feldman&Cousins technique (see Section V of [22]), obtained by adding *ad hoc* systematic error evaluations;
- a full correlation matrix based on the full Monte Carlo simulation including the reconstruction of the simulated data;
- a new approach based on the profile CLs, similar to that used in the Higgs boson discovery [23].

Throughout the analyses the detector configuration defined in Table 2 was considered.

	Fiducial Mass (ton)	Baseline (m)
Near	297	110
Far	693	710

Table 2: Fiducial mass and baselines for Near and Far detectors.

Given the relevance of the CCQE component, arising from the convolution of flux and cross–sections, our analysis makes use of the muon momentum as estimator. The neutrino energy E is obtained either by the usual formula in the CCQE approximation

$$E = \frac{E_\mu - m_\mu^2/(2M)}{1 - (E_\mu - p_\mu \cos \theta)/M}, \quad (2)$$

(M being the nucleon mass, and E_μ, p_μ the muon energy and momentum, respectively) or via Monte Carlo simulation.

For all analyses the two–flavor neutrino mixing in the approximation of one mass dominance is considered, The oscillation probability is given by the formula:

$$P = \sin^2(2\theta_{new}) \sin^2(1.27 \Delta m_{new}^2 L(\text{km})/E(\text{GeV})) \quad (3)$$

where Δm_{new}^2 is the mass splitting between a new heavy–neutrino mass–state and the heaviest among the three SM neutrinos, and θ_{new} is the corresponding mixing angle. As the baseline, L , is fixed by the experiment location, the oscillation is naturally driven by the neutrino energy, with an *amplitude* determined by the mixing parameter.

The disappearance of muon neutrinos due to the presence of an additional sterile state depends only on terms of the extended PMNS [24] mixing matrix ($U_{\alpha i}$ with $\alpha = e, \mu, \tau$ and $i = 1, \dots, 4$) involving the ν_μ flavor state and the additional fourth mass eigenstate. In a 3+1 model at Short Baseline (SBL) we have:

$$P(\nu_\mu \rightarrow \nu_\mu)_{SBL}^{3+1} = 1 - \left[4|U_{\mu 4}|^2(1 - |U_{\mu 4}|^2) \right] \cdot \sin^2 \frac{\Delta m_{41}^2 L}{4E}, \quad (4)$$

where $4|U_{\mu 4}|^2(1 - |U_{\mu 4}|^2)$ results as an *amplitude*.

In contrast, appearance channels (i.e. $\nu_\mu \rightarrow \nu_e$) are driven by terms that mix up the couplings between the initial and final flavour states and the sterile state yielding a more complex picture:

$$P(\nu_\mu \rightarrow \nu_e)_{SBL}^{3+1} = 4|U_{\mu 4}|^2|U_{e 4}|^2 \sin^2 \frac{\Delta m_{41}^2 L}{4E} \quad (5)$$

This holds also in extended $3 + n$ models.

It is interesting to notice that the appearance channel is suppressed by two more powers in $|U_{\alpha 4}|$. Furthermore, since ν_e or ν_μ appearance requires $|U_{e 4}| > 0$ and $|U_{\mu 4}| > 0$, it should be naturally accompanied by a corresponding ν_e and ν_μ disappearance. In this sense the disappearance searches are essential for providing severe constraints on the models of the theory (a more extensive discussion on this issue can be found e.g. in Sect. 2 of [25]).

It must also be noted that the number of ν_e neutrinos depends on the $\nu_e \rightarrow \nu_s$ disappearance and $\nu_\mu \rightarrow \nu_e$ appearance, and, obviously, from the intrinsic ν_e contamination in the beam. On the other hand, the amount of ν_μ neutrinos depends only on the $\nu_\mu \rightarrow \nu_s$ disappearance and $\nu_e \rightarrow \nu_\mu$ appearance but the latter is much smaller due to the fact that the ν_e contamination in ν_μ beams is usually at the percent level. Therefore in the ν_μ disappearance channel the oscillation probabilities in both Near and Far detectors can be measured without any interplay of different flavours, i.e. by the same probability amplitude.

The distributions of events, either in the E_ν or the p_μ variables, normalized to the expected luminosity in 3 years of data taking at FNAL–Booster, or 6.6×10^{20} p.o.t., are reported in Fig. 4.

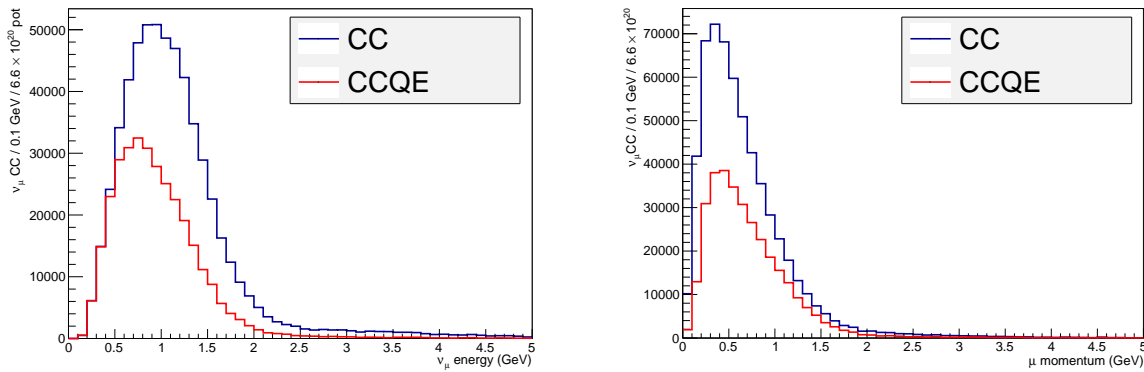


Figure 4: The absolute number of ν_μ CC interactions seen by the Far detector at 710 m, as a function of the E_ν (left) and the p_μ (right). The sub-sample corresponding to the CCQE component is also shown.

3.1. Sensitivity Analysis

Three different ways of evaluating the sensitivity region for sterile neutrinos were applied. On top of the standard sensitivity analysis based on Feldman&Cousins two more refined analyses have been applied:

- matrix-correlation,
- CLs profile likelihood.

In the first one we implemented different smearing matrices for two different observables, the muon *range* and the *number of crossed planes*, associated with the true incoming neutrino energy. These matrices were obtained through a full Monte Carlo simulation.

We studied the sensitivity to the ν_μ disappearance using two different observables: the range and the number of planes at Near and Far detector, evaluated using GLOBES [26].

The ν_μ disappearance can be observed either by a deficit of events (normalization) or, alternatively, by a distortion of the observable spectrum (shape) which are affected by systematic uncertainties expressed by the normalization

errors matrix and the shape errors matrix, respectively. The shape errors matrix represents a migration of events across the bins. In this case the uncertainties are associated with changes not affecting the total number of events and so a depletion of events in some region of the spectrum should be compensated by an enhancement in others. Details of the model used for the shape error matrix can be found in [11].

By applying the frequentist method the χ^2 statistic distribution has been looked at in order to calculate the sensitivity to oscillation parameters. The sensitivity computed considering CC and NC events is almost the same as the sensitivity obtained with only CC events (see Section 12.2 in [11]) and therefore NC background events do not affect the result.

Different cuts on the range and on the number of planes were applied. Sensitivity plots were computed by introducing bin-to-bin correlated systematic uncertainties as expressed in the covariance matrix by considering either 1% correlated error in the normalization or 1% correlated error in the spectrum shape.

As a representative result the sensitivity calculated considering 1% correlated error in the shape is plotted in Fig. 5. It is interesting to outline that the systematic error on normalization affects the sensitivity region only at the extreme edges at small values of the mixing angle parameter.

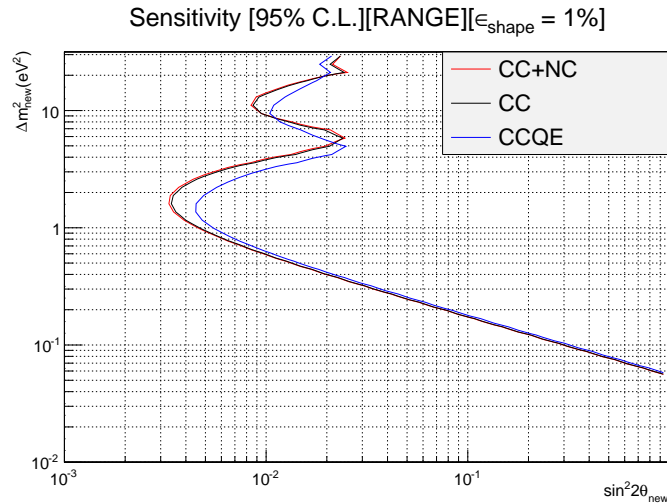


Figure 5: 95% CL sensitivity obtained using range for all (QE, Res, DIS) CC (black) and CC+NC (red) events and for only CCQE events (blue). In this case we considered 1% bin-to-bin correlated error in the shape.

In the profile CLs method we introduce a new test-statistics that depends on a *signal-strength* variable. We may observe that, by looking at Eq. 3, for a fixed Δm_{new}^2 , the first factor, $\sin^2(2\theta_{new})$, acts as an amplification quantity of the configuration shape of the estimator being used. Then, we may identify the signal-strength μ with $\sin^2(2\theta_{new})$ and construct the estimator function:

$$f = \frac{1 - \mu \cdot \sin^2(1.27 \Delta m_{new}^2 L_{Far}/E)}{1 - \mu \cdot \sin^2(1.27 \Delta m_{new}^2 L_{Near}/E)} \quad (6)$$

In a simplified way, for each Δm_{new}^2 a sensitivity limit can be obtained from the *p-value* of the distribution of the estimator in Eq. 6, in the assumption of *background-only* hypothesis.

That procedure does not correspond to computing the exclusion region of a signal, even if it provides confidence for it. The exclusion plot should be obtained by fully developing the CL_S procedure as outlined above. However, since we are first interested in exploiting the sensitivity of our experiment to any oscillation pattern not compatible with the standard 3-neutrino scenario, the above procedure provides insights into such question, and it is fully compatible with the previous two analyses and the usual neutrino analysis found in literature.

Moreover, following the same attitude, an even more *aggressive* procedure can be applied. Since the deconvolution from p_μ to E_ν introduces a reduction of the information, we investigate whether the more direct and measurable

parameter, p_μ , is a valuable one. In such a case Eq. 6 becomes:

$$f = \frac{1 - \mu \cdot \sin^2(1.27 \Delta m^2 L_{Far}/p_\mu)}{1 - \mu \cdot \sin^2(1.27 \Delta m^2 L_{Near}/p_\mu)} \quad (7)$$

The sensitivity plot in Fig. 6 actually provides an “effective” sensitivity limit in the “effective” variables Δm^2 and the reconstructed muon momentum, $p_{\mu,rec}$. We checked that the “effective” Δm^2 is simply scaled-off towards higher values, not affecting the mixing angle limit. This is the best sensitivity result that our experiment can achieve if the systematics can be limited to 1% level, as we are confident in. A sensitivity to mixing angles in $\sin^2(2\theta_{new})$ below 10^{-2} can therefore be obtained in a large region of Δm^2 , around the 1 eV² scale.

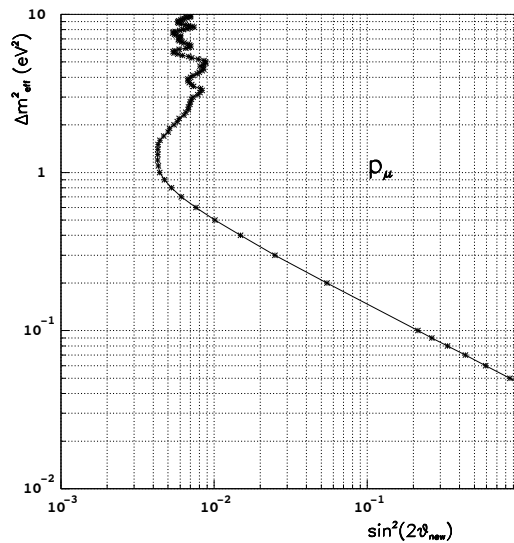


Figure 6: The sensitivity plot obtained by computing the modified raster-scan method, in a CL_S framework, and by using the reconstructed muon momentum as estimator. A conservative cut of $p_{\mu,rec} \geq 500$ MeV was applied.

4. Conclusions

Existing anomalies in the neutrino sector may hint to the existence of one or more additional *sterile* neutrino families. We performed a detailed study of the physics case in order to set a Short-Baseline experiment at the FNAL-Booster neutrino beam to exploit the measurement of the charged current events. An independent measurement on ν_μ , complementary to the already proposed experiments on ν_e , is mandatory to either prove or reject the existence of sterile neutrinos, even in case of null result for ν_e . Moreover, very massive detectors are mandatory to collect a large number of events and therefore improve the disentangling of systematic effects.

The best option in terms of physics reach and funding constraints is provided by two spectrometers based on dipoles iron magnets, at the Near and Far sites, located at 110 and 710 m from the FNAL-Booster neutrino source, respectively, possibly placed behind the proposed LAr detectors. In this way we will succeed to keep the systematic error at the level of $1 \div 2\%$ for the measurements of the ν_μ interactions, in particular the measurement of the muon-momentum at the percent level and the identification of its charge on event-by-event basis, extended to well below 1 GeV.

We plan to perform a full re-use of the OPERA spectrometers that will be dismantled starting at the end of 2015. Each site at FNAL will host a part of the two coupled OPERA magnets, based on well know technology allowing to realize “clone” detectors at the Near and Far sites. The spectrometers will make use of RPC detectors, already available, which have demonstrated their robustness and effectiveness.

Acknowledgements

We warmly thank the organizers of ICHEP2014 for the kind invitation to report about the proposal of the NESSiE Collaboration at the FNAL–Booster neutrino–beam.

References

- [1] DAYA–BAY Collaboration, F. An et al., Phys. Rev.Lett. 108, 171803 (2012), arXiv:1203.1669; RENO Collaboration, J. Ahn et al., Phys. Rev.Lett. 108, 191802 (2012), arXiv:1204.0626; DOUBLE–CHOOZ Collaboration, Y. Abe et al., Phys. Rev. Lett. 108, 131801 (2012), arXiv:1207.6632; T2K Collaboration, K. Abe et al., Phys. Rev.Lett. 107, 041801 (2011), arXiv:1106.2822.
- [2] B. Pontecorvo, Zh. Eksp. Teor. Fiz. 53, 1717 (1967) [Sov. Phys. JETP 26, 984 (1968)].
- [3] K.N. Abazajian et al., “*Light Sterile neutrinos: a White Paper*”, (2012), arXiv:1204.5379.
- [4] J. Kopp, P. A. N. Machado, M. Maltoni, and T. Schwetz, JHEP 05, 050 (2013), arXiv:1303.3011; T. Schwetz, Nuclear Physics B, vol. 235-236, pp. 2292235, 2013; C. Giunti, M. Laveder, Y. F. Li, Q. Y. Liu, and H. W. Long, Phys. Rev. D, vol. 86, no. 11, Article ID 113014, 2012.
- [5] A. Sousa (MINOS) and R. Wendell (Super–K) contributions at Neutrino2014, Boston, USA, 2-7 June 2014.
- [6] M. Netti et al., <https://edms.cern.ch/nav/P:CERN-0000077383:V0/P:CERN-0000096728:V0/TAB3>.
- [7] P5 reports in <http://science.energy.gov/hep/hepap/reports/>.
- [8] MicroBooNE Experiment, <http://www-microboone.fnal.gov/>.
- [9] ICARUS Collaboration, M. Antonello et al., arXiv:1312.7252.
- [10] LAr1–ND Collaboration, C. Adams et al., P–1053, 31 December 2013 and arXiv:1309.7987v3.
- [11] NESSiE Collaborations, A. Anokhina et al., FNAL–P–1057, arXiv:1404.2521.
- [12] CDHS Collaboration, F. Dydak et al., Phys. Lett. **B134**, 281 (1984).
- [13] MiniBooNE Collaboration, A. A. Aguilar–Arevalo et al., Phys. Rev. Lett. 103, 061802 (2009), arXiv:0903.2465.
- [14] MiniBooNE and SciBooNE Collaborations, K. B. M. Mahn et al., Phys. Rev. D85, 032007 (2012), arXiv:1106.5685; G. Cheng et al., Phys. Rev. D86, 052009 (2012), arXiv:1208.0322.
- [15] CCFR Collaboration, I. E. Stockdale and A. Bodek, F. Borcherding, N. Giokaris, K. Lang, K. et al, Phys.Rev.Lett. **52** 1384 (1984).
- [16] NESSiE Collaboration, P. Bernardini et al., SPSC–P–343 (2011), arXiv:1111.2242.
- [17] ICARUS and NESSiE Collaborations, M. Antonello et al., SPSC–P–347 (2012), arXiv:1203.3432.
- [18] L. Stanco et al., AHEP 2013 (2013) ID 948626, arXiv:1306.3455v2.
- [19] J. R. Sanford and C. L. Wang (1967), BNL Internal Report, BNL–11479; MiniBooNE Collaboration, A. A. Aguilar–Arevalo et al., Phys. Rev. D79, 072002 (2009), arXiv:hep-ex/0601022v1 (2006).
- [20] G. Battistoni et al., AIP Conf. Proc. **896**, 31 (2007).
- [21] The OPERA collaboration, R. Acquafredda et al., JINST **4** 4018 (2009).
- [22] G. J. Feldman and R. D. Cousins, “*Unified approach to the classical statistical analysis of small signals*”, Phys. Rev. D57, 3873 (1998), <http://arxiv.org/abs/physics/9711021v2>.
- [23] ATLAS and CMS Collaborations, LHC Higgs Combination Group, ATL-PHYS-PUB-2011-1, CMS NOTE-2011/005,
- [24] B. Pontecorvo, Sov. Phys. JETP 26, 984 (1968); Z. Maki, M. Nakagawa, and S. Sakata, Prog. Theor. Phys. 28, 870 (1962).
- [25] W. Winter, Phys. Rev. D85, 113005 (2012), arXiv:1204.2671.
- [26] <http://www.mpi-hd.mpg.de/personalhomes/globes/index.html>.